Hindawi
Shock and Vibration
Volume 2023, Article ID 5582345, 21 pages
https://doi.org/10.1155/2023/5582345

Research Article

Study on Mechanism and Main Influencing Factors of Rockburst under Complex Conditions of Hard and Deep Overburden

Ma Xingen,[1,2] **Pan Jun**,[3] **Zou Qinghai**,[3] **Li Yongyuan**,[2] **Feng Fan**,[3] **Wang Huifeng**,[2] **Ye Xiangping**,[3] **Gong Yongchun**,[3] **and Mou Biao**[3]

[1]*China University of Mining and Technology, Xuzhou 221000, China*
[2]*Huaneng Coal Technology Research Co., Ltd., Beijing 100070, China*
[3]*Xinzhuang Coal Mine of Huaneng Qingyang Coal Power Co., Ltd, Qingyang 745000, China*

Correspondence should be addressed to Ma Xingen; 294185559@qq.com

Received 14 June 2023; Revised 22 October 2023; Accepted 26 October 2023; Published 13 November 2023

Academic Editor: Antonio Giuffrida

Copyright © 2023 Ma Xingen et al. This is an open access article distributed under the Creative Commons Attribution License, which permits unrestricted use, distribution, and reproduction in any medium, provided the original work is properly cited.

Xinzhuang Coal Mine is a typical kilometer-deep rockburst mine in the Ningzheng mining area of China Huaneng Group, which is still in the capital construction period. At present, there are a few studies on the rockburst mechanism and prevention of this mine. In order to explore the occurrence mechanism and main influencing factors of rockburst under the complex geological conditions of large buried depth, thick topsoil, and hard overburden in Xinzhuang Coal Mine, this paper, based on the analysis of the basic geological data of the mine, deeply explores the comprehensive disaster factors of Xinzhuang Coal Mine; then, uses the analytic hierarchy process to carry out quantitative analysis of each disaster factor, and finally, it obtains the impact type and occurrence mechanism of the mine. Through research, it is found that the main disaster factors of Xinzhuang Coal Mine are mining depth, coal seam thickness, coal seam thickness change, tectonic stress field, hard overburden, roadway layout, bottom coal reservation, and tunneling activities. The key to the process of the rockburst disaster in Xinzhuang Coal Mine is the superimposed effect of static and dynamic loads on the roadway surrounding the rock system. The potential rockburst type during excavation and mining is the "high static and dynamic load disturbance" type.

1. Introduction

Coal is the main primary energy in China and plays an irreplaceable role in the development of the national economy [1]. However, with the increasing depth and production intensity of coal mining in China, the threat of rockbursts faced by coal mines is becoming increasingly serious [2]. At present, there are more than 130 rockburst mines in China. In recent years, major rockburst accidents have occurred in Shandong Longyun Coal Mine (October 20, 2018), Jilin Longjiapu Coal Mine (June 9, 2019), Hebei Tangshan Coal Mine (August 2, 2019), Shandong Xinjulong Coal Mine (February 22, 2020), and Shaanxi Hujiahe Coal Mine (October 11, 2021), causing serious casualties and economic losses [3]. Rockbursts have become one of the main dynamic disasters faced by deep coal mining in China [4, 5].

The mechanism of rockburst disasters is complex, and monitoring and warning are difficult. Onsite prevention and control must strictly follow the principle of "one mine, one policy. One side, one policy [6, 7]." At present, a large number of scholars have conducted considerable research on the mechanism, monitoring and warning, and prevention measures of rockbursts. For example, Professor Dou Linming's team has introduced SOS microvibration monitoring technology from Poland and gradually achieved independent software and hardware development [8]. Researcher Qi Qingxin proposed the "three factors" mechanism of rockburst after analyzing and studying the failure characteristics of typical rockburst mines [9].

Professor Pan Yishan proposed the energy criterion and disturbance impact criterion for the initiation of rockburst after analyzing the entire process of rockburst occurrence [10]. Professor Jiang Fuxing's team proposed an energy dissipation index to evaluate the effectiveness of coal seam pressure relief and derived a quantitative calculation method for rockburst control drilling parameters based on the energy dissipation index [11]. Kaiser's team proposed the support principle for rockburst tunnels and developed rockburst tunnel support design software [12]. Mottahedi et al. obtained a probability prediction model and method for coal mine rockburst disasters through research, and Simser BP proposed a systematic prevention and management method for rockburst mines [13, 14]. On the basis of in-depth research by a large number of scholars, a relatively complete system for preventing and controlling rockbursts has been preliminarily established in the industry, which has basically achieved the prevention and control of coal mine rockbursts nationwide [15]. However, due to the complexity of rockburst, there are still many problems such as "low efficiency, poor safety, and high cost" in onsite prevention and control. The fundamental reason for this is insufficient research on the key theories and differences of rockburst occurrence mechanisms and prevention and control technologies in various mines [16, 17].

Xinzhuang Coal Mine is a kilometer deep mine located in the Ningzheng mining area of China Huaneng Group, with a planned production capacity of 8 million tons per year. It is a typical rockburst mine. At present, the mine is still in the infrastructure construction period, and there is relatively little research on the prevention and control of rockbursts in the mine. Conducting relevant research during the mine construction period has extremely important practical significance for the current tunnel layout, excavation, and subsequent safety production guidance. Therefore, this paper focuses on the complex geological conditions of large burial depth, thick topsoil, and hard overburden in Xinzhuang Coal Mine and conducts research on the mechanism and main influencing factors of rockburst occurrence in the mine, in order to provide theoretical reference for the prevention and control of rockburst in the mine and similar mines. Based on the mining experience of neighboring mining areas (such as Binchang Mining Area and Linbei Mining Area), the mining in this area is facing a serious threat of rockburst disaster. Therefore, it is necessary to start researching and formulating corresponding prevention and control measures as soon as possible. This study is the initial stage of research on the prevention and control of rockbursts in Xinzhuang Coal Mine, including the mechanism and main influencing factors. At the current research stage, due to the influence of mine construction and mining plans, there is a lack of a large amount of research data support. Therefore, a preliminary analysis of the influencing factors can only be conducted from a macroperspective. Based on this study, a preliminary plan for mine erosion prevention can be formulated, and in the subsequent actual mining process, it can be gradually explored and optimized to form a complete prevention and control system.

2. Overview of Mine Engineering

2.1. Overview of Xinzhuang Coal Mine. The Ningzheng mining area of Huaneng Group is located in the southern exploration area of Ningxiang County, including two trial productions and under construction mines: Hetaoyu Coal Mine and Xinzhuang Coal Mine. The planned annual production capacity of both mines is 8 million tons per year, and the minefield relationship plan is shown in Figure 1. The mining area is a concealed and fully covered coal field with quaternary strata, and the burial depth of coal-bearing strata is generally below 700 m. The Yan'an Formation in the mining area contains three minable coal seams: coal 2, coal 5, and coal 8, which are located in the upper, middle, and lower coal-bearing sections of the Yan'an Formation from top to bottom. Coal 2 and coal 5 are relatively stable minable coal seams in the minable area. Judging from the entire mining area, they are unstable locally minable coal seams. Coal 8 is a relatively stable main minable coal seam in the entire area and is also the first designed coal seam for the two mines in the mining area.

The Xinzhuang minefield is approximately 20.0 km long from east to west, 7.6–12.5 km wide from north to south, and covers an area of 206.2823 km^2. Among them, the mining elevation of Xinzhuang Coal Mine is −40~+300 m, the ground elevation is +1121.6 m, the mining depth is up to kilometers, and the ground pressure is high. The rock strength of the coal seam roof and floor is low, and the rock is prone to deformation. The resulting cracks cause groundwater infiltration, leading to a further reduction in rock strength and poor overall stability of the surrounding rock. The main roadway has a large length and cross-section, making support difficult.

The Xinzhuang Coal Mine mainly mines coal 8 layer, located in the first section of the Yan'an Formation. The layers are stable, with a burial depth of 653.97~1248.78 m, a minable thickness of 0.88~27.42 m, and an average thickness of 8.71 m. The coal-bearing area is 166.16 km^2, the minable area is 158 km^2, and the estimated resource area is 157.14 km^2. The ultrathick coal seams are mainly distributed in the axis of the Xinzhuang syncline and Qiaojiamiao syncline, with thick coal seams, medium-thick coal seams, and thin coal seams distributed symmetrically along the two wings of the syncline. The minable area accounts for 95% of the coal seam distribution area and 77% of the minefield area.

In addition, from the construction situation of adjacent mines such as Hetaoyu Coal Mine and Gaojiapu Coal Mine, it can be seen that after entering the production stage, the mine in this area is prone to deformation such as roof fall and floor heave in the bottom parking lot and main roadway due to high ground pressure (shown as Figure 2). The Xinzhuang and Hetaoyu minefields are adjacent, with similar geological and coal seam occurrence conditions. It is expected that the mine will also face similar problems after production.

2.2. Fundamentals of Rockburst Research. Xinzhuang Coal Mine has conducted a ground stress test and identified the rockburst tendency of the coal 8 layer. The ground stress test results are shown in Table 1. The maximum horizontal

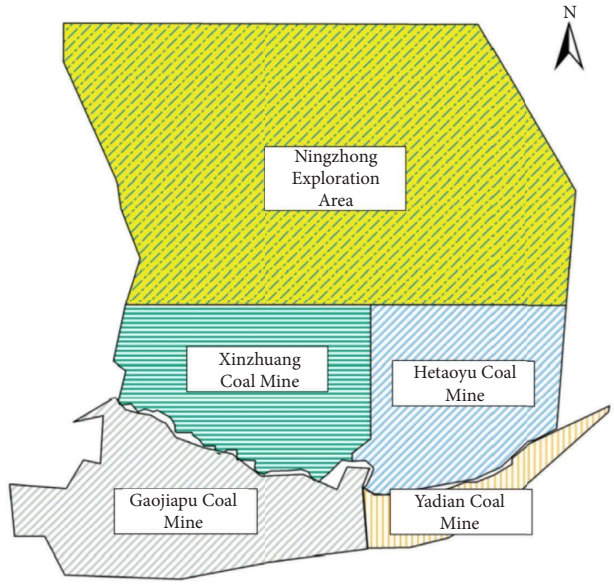

Figure 1: Minefield relationship diagram.

(a) (b)

Figure 2: Photo of tunnel deformation in Hetaoyu coal mine. (a) Auxiliary transportation lane. (b) Auxiliary transportation stone gate.

principal stress directions of the three groups of test points are N41.5° E, N32.8° E, and N43.8° E, respectively. The dominant direction of the maximum horizontal principal stress is NNE, with good consistency in direction. On the whole, the ground stress fields of three groups of measuring points in Xinzhuang Coal Mine belong to a high-stress value area (>18 MPa) in terms of the measurement value and show obvious deep ground stress distribution characteristics.

The identification results of the rockburst tendency of coal 8 layer, coal 8 roof, and coal 8 floor in Xinzhuang Coal Mine are shown in Tables 2 and 3, respectively. According to the "National Standard of the People's Republic of China-Determination of Rockburst Tendency Standard" (GB/T25217.1-2010), it can be seen that the coal 8 layer has a weak rockburst tendency, coal 8 roof has no rockburst tendency, and the coal 8 floor has a weak rockburst tendency [18].

3. Analysis of Comprehensive Disaster Causing Factors

The geological conditions of Xinzhuang Coal Mine are complex, with the most prominent features being large burial depths and hard overlying rock. The large burial depths directly lead to high ground stress in the surrounding rock of the tunnel, while the hard overlying rock can easily cause a suspended roof in the goaf after mining, making it

Table 1: Ground stress test results.

Measure point	Maximum horizontal principal stress (MPa)	Minimum horizontal principal stress (MPa)	Vertical stress (MPa)
1	26.93	13.68	24.17
2	25.23	13.88	24.38
3	24.94	13.36	24.19

Table 2: Test result of the rockburst tendency of coal 8 in Xinzhuang Coal Mine.

Uniaxial compressive strength (MPa)	Dynamic failure time (ms)	Impact energy index	Elastic energy index
13.963	1246	2.483	12.522

Table 3: Test result of rockburst tendency of coal 8 roof and floor in Xinzhuang Coal Mine.

Type	Item				
	Load (MPa)	Apparent density ($kg \cdot m^{-3}$)	Elastic modulus (GPa)	Tensile strength (MPa)	Bending energy index (kJ)
Roof	0.078	2.548	7.584	2.460	4.277
Floor	0.288	2.585	10.047	3.343	48.253

difficult for the roof to collapse after mining and causing a significant disturbance during the collapse. High ground stress and strong collapse disturbance bring great possibilities for the occurrence of rockbursts.

During the tunneling of the main roadway in panel 1 of Xinzhuang Coal Mine, there have been many strata pressure appearances, especially in the area near the intersection of the roadway and tectonics. The preliminary statistics are shown in Table 4. In addition to the locations where the mine pressure appears in the table, there are also slight floor heaves in other tunnels, posing a threat to the safety of mine production and the lives and property of workers. Although Xinzhuang Coal Mine has taken a series of measures to monitor and prevent mine pressure and has achieved certain results, forming a relatively systematic method for monitoring and controlling strong mine pressure is difficult. However, due to the unique nature of the mine structure, mine pressure manifestations still occur frequently. It is urgent to analyze the influencing factors of rockbursts and propose targeted control technologies [19, 20]. Therefore, according to engineering experience and statistical judgment, based on the "Detailed Rules for the Prevention and Control of Coal Mine Rockburst" and the "Interim Measures for the Appraisal of Rockburst Mines" of China, this section first analyzes the influencing factors of rockburst during the excavation of the main roadway in Xinzhuang Coal Mine.

3.1. Analysis of Disaster Factors Caused by Mining Depth. Based on the exploration drilling data of Xinzhuang Coal Mine, a contour map of the buried depth of the coal 8 layer is summarized and analyzed, as shown in Figure 3.

Under the condition of large burial depth, the self-weight stress field is significant and the important component in the influence of static load is the original rock stress field. The stress field of the original rock, which is not disturbed by the mining project before the mining activities, is carried out, mainly formed by the self-weight stress field formed by the self-weight of the coal and rock mass and the tectonic stress field generated by the tectonic movement. The self-weight stress field is mainly determined by the mining depth. As the mining depth increases, the self-weight stress in the coal seam increases and the elastic energy accumulated in the coal rock mass also increases, thereby increasing the possibility of rockburst disasters [21, 22].

According to the existing research results, the initial mining depth of rockburst is [23] as follows:

$$H \geq 1.73 \frac{R_c}{\gamma} \sqrt{\frac{K_0}{C}}, \tag{1}$$

where R_c is the uniaxial compressive strength of coal, γ is the density of coal, K_0 represents the coefficient, which is greater than 1, $C = (1\text{-}2\mu)\ (1+\mu)^2/(1\text{-}\mu)^2$, and μ stands for Poisson's ratio.

Based on the physical and mechanical properties of coal and rock in Xinzhuang Coal Mine ($R_c \approx 14$ MPa, $\gamma = 1.39 \times 10^3$ kg/m^3, $K_0 = 3$, $\mu = 0.47$, $C = 0.46$), the initial mining depth of rock burst is approximately calculated (H = 445 m).

The burial depth of the coal 8 layer in Xinzhuang Coal Mine is 653.97~1248.78 m, which is in the stage of a sharp increase in the probability of rockburst occurrence. The impact of mining depth factors on the rockburst risk in Xinzhuang Coal Mine cannot be ignored.

3.2. Coal Seam Thickness. The compressive strength and deformation characteristics of coal seams and rock layers are different, so the bearing capacity of thicker areas of coal seams is weaker, while the bearing capacity of thinner areas

Table 4: Appearance of mine pressure in Xinzhuang Coal Mine.

Number	Location of mining pressure manifestation	Situation description
1	Central west auxiliary transportation lane 3-4 link lane (mileage 996–1361 m)	The floor bulges and multiple fractures occur on both sides of the tunnel
2	Central west auxiliary transportation lane 6-7 link lane (mileage 2275–2820 m)	Bottom plate ruptures
3	Central belt main lane 2-3 link lane (mileage 679–1043 m)	Tunnel floor bulges

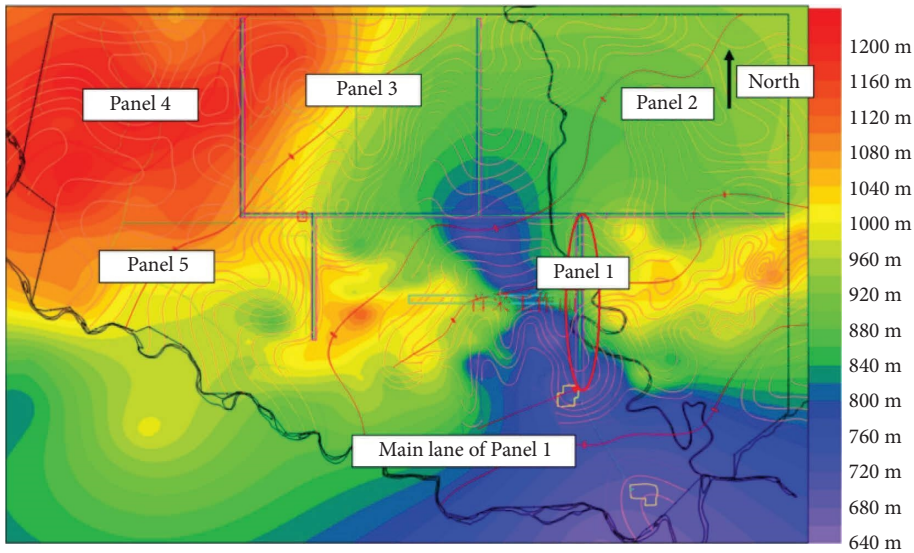

Figure 3: Contour map of coal 8 layer buried depth.

of coal seams is stronger. This also leads to changes in the distribution of in-situ stress in areas where coal seam thickness changes, and uneven stress distribution is one of the causes of impact disasters.

The risk level of rockburst disasters is closely related to the thickness and changes of coal seams: the thicker the coal seam, the greater the risk of impact disasters. At the same time, areas with sudden changes in coal seam thickness are often prone to rockbursts due to increased support pressure [24]. The maximum thickness of the coal 8 seam in Xinzhuang Coal Mine has reached over 20 m, with an average thickness of 8.50 m. It belongs to an extremely thick coal seam, so the influence of coal seam thickness on strong mining pressure cannot be ignored.

In addition, the influence of changes in coal seam thickness on the formation of strong rock pressure is often more important than the thickness itself. At locations with changes in thickness, strong rock pressure is often prone to occur, as the support pressure in these areas increases. The influence of different changes in the local thickness of coal seams on the stress field is as follows [25, 26].

(1) The effects of local thinning and thickening of coal seam thickness are different. When the thickness of the coal seam is thinned locally, the vertical crustal stress will increase in the thin part of the coal seam. When the thickness of the coal seam locally thickens, the vertical crustal stress will decrease in the thick part of the coal seam, while the vertical crustal stress will increase in the normal thickness part on both sides of the thick part of the coal seam. Moreover, local thinning and thickening of coal seams result in varying degrees of stress concentration. (2) The more severe the change in coal seam thickness, the higher the degree of stress concentration. (3) When the coal seam becomes thinner, the shorter the thinning part, the greater the stress concentration coefficient. (4) The degree of stress concentration in the local variation area of coal seam thickness is related to the difference in elastic modulus between the coal seam and the roof and floor, that is, the larger the difference, the higher the degree of stress concentration.

The Xinzhuang Coal Mine mainly mines the coal 8 layer, and its thickness and changes are shown in Figure 4. According to the contour map of the thickness of the coal 8 layer, the thickness mainly varies within the range of 1.5~23 m. Overall, the change in coal thickness is relatively gentle, but in some areas, especially in folded areas, the thickness of coal seams varies significantly. Specific areas include the Qiaojiamiao syncline area west of the main roadway in panel 1, the area near the boundary of the southeast panel in panel 2, and the Liubao anticline area in the east of the fourth panel. The stress concentration in areas with drastic changes in coal seam thickness is relatively high. In the subsequent process of a roadway or working face layout, consideration should be given to avoiding these areas or taking corresponding measures to reduce the stress concentration in the surrounding coal and rock masses.

3.3. Geological Structure. The main influencing factor of mine structural stress field is geological structure. Geological structures can change the distribution of local ground stress, leading to local stress concentration. The uneven distribution and local concentration of ground stress are one of the causes of rockburst disasters.

The distribution of fold structures in Xinzhuang Coal Mine is shown in Figure 5. From the figure, it can be seen that the Xinzhuang Coal Mine is located in a folded structure area as a whole, with a total of 5 large folds, each consisting of two uplifts or depressions. The dip angles of the two wings of the anisotropic anticline are extremely gentle, generally around 4-5°, and the strike of each fold axis is in an inverse "S" shape. The vicinity of each fold structure area is prone to rockburst disasters.

The overview of 5 folds is as follows:

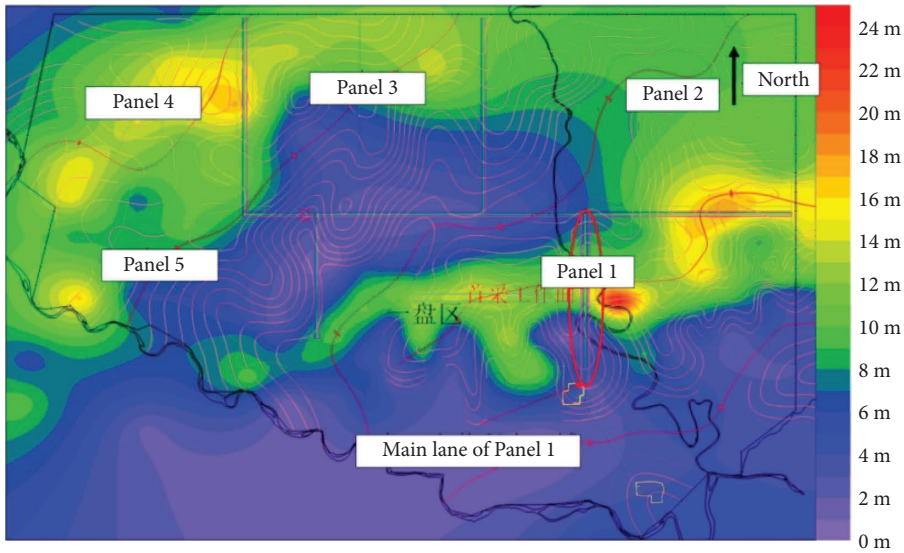

Figure 4: Contour map of coal 8 layer thickness.

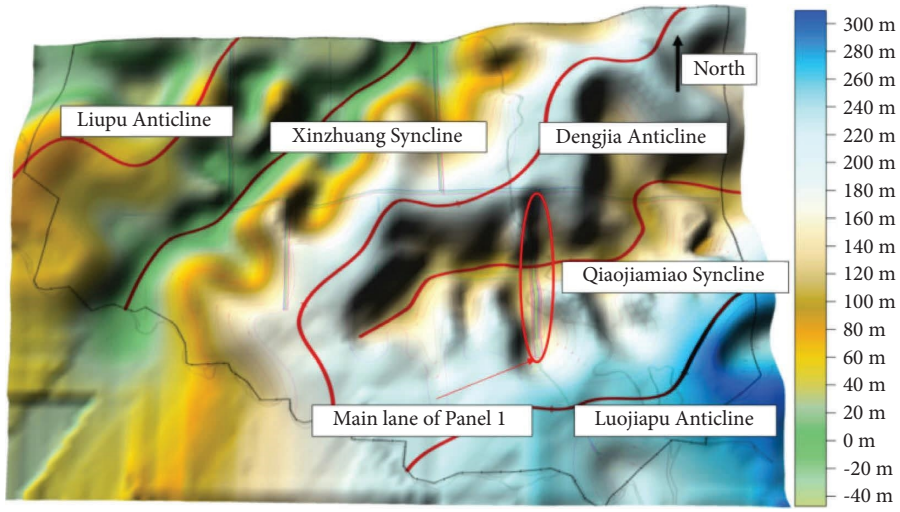

Figure 5: Three-dimensional schematic diagram of coal 8 layer occurrence.

(1) Liupu anticline: located in the northwest angle of the exploration area, plunging southward, extending about 7.5 km in the area, it can be divided into two uplifts, and the thickness of Yan'an Formation in the uplifted area is less than 20 m.

(2) Xinzhuang syncline: the area extends about 9 km and is roughly composed of two depressions. The thickness of the Yan'an Formation in the depression area is greater than 80 m.

(3) Dengjiaanticline: located in the central part of the exploration area, it passes through the exploration area in an undulating shape and extends northward to connect with the Xitou anticline in the central exploration area of Ningxiang County. The extension length within the area is about 12 km, and the axis of the uplift lacks the Yan'an Formation and coal seams. The central axis of the anticline is relatively concave with thin coal seam deposits in the saddle.

(4) Qiaojiamiaosyncline: located in the early mining area in the eastern part of the exploration area, it is clearly distributed in a serpentine shape and generally extends in a northeast direction. There are roughly two depressions, with a thickness of over 70 m in the Yan'an Formation and a maximum thickness of 83.17 m.

(5) Luojiapu anticline: extending eastward to the southern exploration area of Zhengning, it is connected to the same name anticline in the area, with the southern wing and axis missing the Fuxian Formation and Yan'an Formation.

3.4. Hard Overlying Rock. The breeding and development of rockburst is a complex nonlinear process, but its physical essence is the transformation of energy [27]. The fracture of the overlying high roof in the mining area and the vibration energy generated during the fracture process are often one of the important factors causing the occurrence of rockburst disasters. The thicker and harder the overlying rock layer, the less energy loss caused by the downward propagation of fractures, and the greater the elastic energy accumulated by the coal and rock below, resulting in a higher risk of rockburst. After excavation activities, the stress in the surrounding rock redistributes. Before the cantilever beam of the hard roof is broken, the suspended area continues to increase and the roof continuously accumulates energy. Also, before the occurrence of rockburst disasters, the surrounding rock is in a state of ultimate equilibrium in the static stress field. When the mining disturbance occurs in the coal mine, the new disturbance stress produces a dynamic load effect on the coal and rock mass in the limit equilibrium state. Under the coupling superposition of the mining disturbance load and the crustal stress static load, the stress superposition result exceeds the critical bearing value of the coal and rock strata, reaching the critical load for the occurrence of coal and rock dynamic disasters, inducing the plastic failure of the coal and rock mass, and leading to the occurrence of roof dynamic disasters.

3.4.1. Impact of Distance between Hard Overlying Rock and Coal Seam on Rockburst. Due to the attenuation of underground energy transmission, the impact of near-field hard overburden fracture on the roadway under the same energy release is much greater than the impact of far-field hard overburden fracture on the roadway. Therefore, this study combines the frequency and energy of microseisms to analyze the impact of the rockburst on the hard rock layer above the coal seam with a thickness of over 10 m.

From Figure 6, it can be seen that the distance between the first layer of thick and hard rock above the coal seam (with a thickness of over 10 m) in the area where the main roadway is located mostly within 40 m to the coal seam, and in some areas, it is even less than 20 m. The distance between the hard overlying rock and the coal seam has a significant impact on the rockburst risk of Xinzhuang Coal Mine.

3.4.2. Impact of Hard Overburden Thickness on Rockburst. According to existing conclusions, the thick and hard rock layers overlying the coal body have a significant impact on the rockburst. According to the statistical results of relevant drilling data, the thickness distribution contour map of the first sandstone layer with thickness greater than 10 m from the upper coal 8 layer is drawn in Figure 7. As shown in the figure, the thickness of the overlying thick sandstone in Xinzhuang Coal Mine is mostly close to 20 m and the thickness of the overlying thick sandstone in some areas can reach up to 40 m. Therefore, the thickness of the hard overlying rock in the upper part of coal 8 in Xinzhuang Coal Mine has a significant impact on the risk of rockburst.

3.5. Tunnel Excavation. The disaster process of Xinzhuang Coal Mine is mainly influenced by the superposition of dynamic and static loads, so the impact of excavation activities is the main part [28, 29]. The dynamic load disturbance caused by excavation causes a redistribution of stress in the coal and rock mass, thereby affecting the original rock stress field. The static load effect of the supporting stress field is superimposed, and then under the disturbance of excavation strength and dynamic load, rockburst disasters occur. The following is an analysis of these influencing factors in combination with onsite mine pressure monitoring and mine pressure activity.

At present, the underground construction of Xinzhuang Coal Mine is still in the development stage. A total of 8 SOS single-component microseismic sensors (SOS-U7) are arranged underground. With the later development of the mine, the number of microseismic sensors will gradually increase to ensure production safety. The layout plan of the existing microseismic sensors in the mine is shown in Figure 8.

With the progress of excavation activities, the mining pressure is in a constantly unstable and stable cycle, and unreasonable excavation intensity can easily disrupt this equilibrium state, leading to rockbursts. This section selects microseismic data ($>10^3$ J) from December 2020 to March 2021 in the main roadway area of the first panel of Xinzhuang Coal Mine for analysis, combined with monthly excavation footage. The evolution diagram is shown in Figures 9–12 (the circles 1–7 in the figure represent the area where the excavation head is located. The particles represent energy events with vibration energy greater than 10^3 J: the blue particles represent energy events between 10^3 J and 10^4 and the yellow particles represent energy events greater than 10^4 J.).

December 2020: the footage of area 1 is 87 m, area 2 is 76.9 m, area 3 is 124.5 m, area 4 is 45.2 m, area 5 is 158.8 m, area 6 is 72 m, and area 7 is 65.5 m. The total monthly footage is 629.9 m, with an average daily footage of 20.3 m. During this period, microseisms with energy greater than 10^3 J occurred 36 times, with an average of 0.057 times per meter and 1.16 times per day.

January 2021: the footage of area 1 is 69.3 m, area 2 is 201.8 m, area 3 is 154 m, and area 4 is 85 m. The total monthly footage is 510.1 m, with an average daily footage of 16.45 m. During this period, a total of 51 microseisms with energy greater than 10^3 J occurred, with an average of 0.099 high energy ($>10^3$ J) microseisms per meter of footage and an average of 1.65 high energy microseisms per day.

February 2021: the footage of area 1 is 12.1 m, area 2 is 87.5 m, area 3 is 11.5 m, area 4 is 21 m, and area 5 is 16.9 m. The total monthly footage is 149 m, with an average daily footage of 5.3 m. During this period, a total of 31 microseisms with energy greater than 10^3 J occurred, with an average of 0.208 high energy ($>10^3$ J) microseisms per meter of footage and an average of 1.11 daily high energy microseisms.

March 2021: the footage of area 1 is 65 m, area 2 is 145 m, area 3 is 100 m, area 4 is 96.2 m, area 5 is 105.2 m, and area 6 is 78.1 m. The total monthly footage is 589.5 m, with an

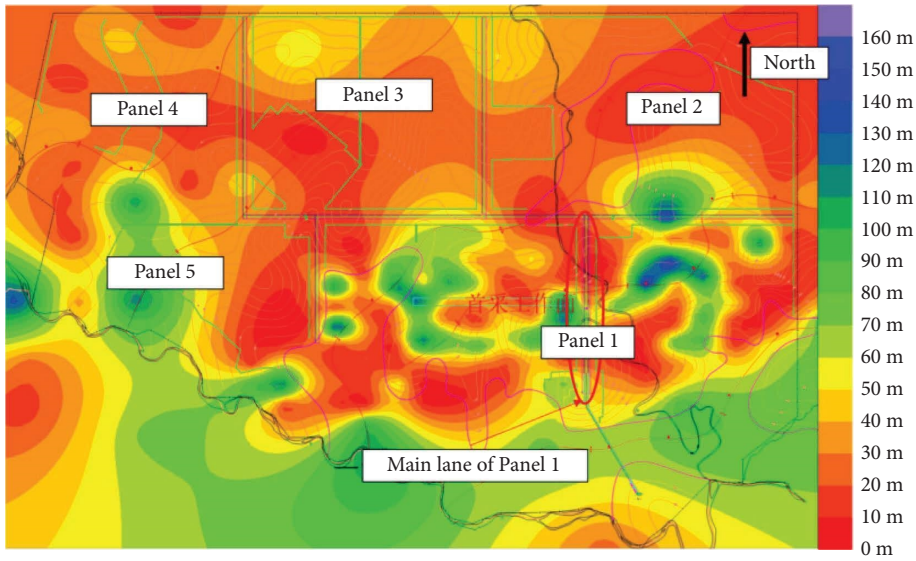

Figure 6: Contour map of the distance between thick rock layers (>10 m) and coal seam.

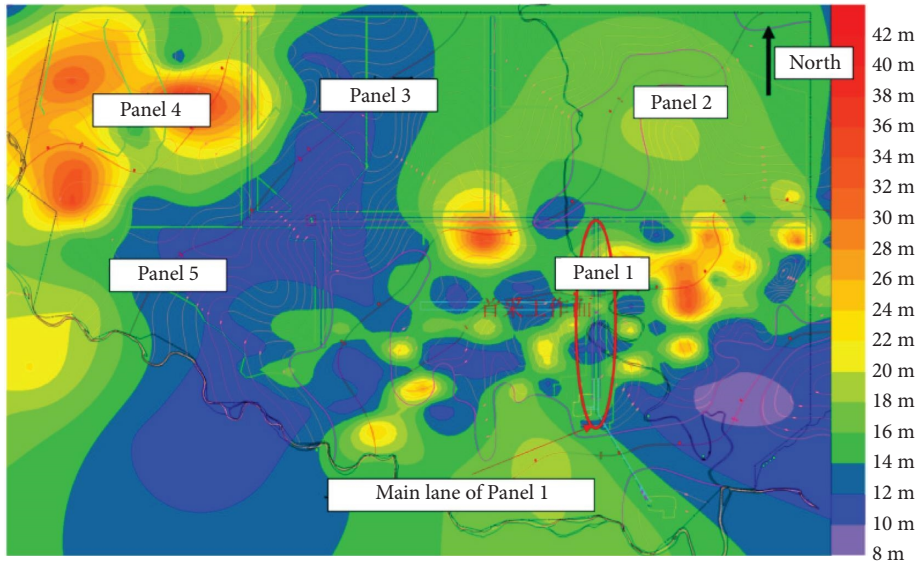

Figure 7: Thickness distribution contour map of the first sandstone layer with a thickness greater than 10 m from the upper coal 8 layer.

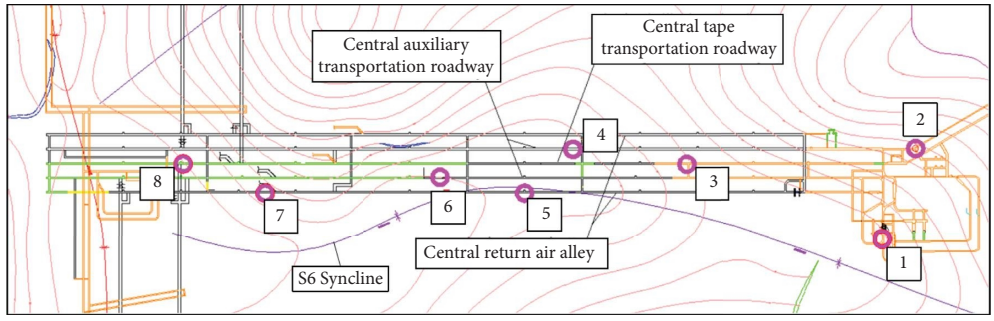

Figure 8: Layout plan of microseismic sensors in Xinzhuang Coal Mine.

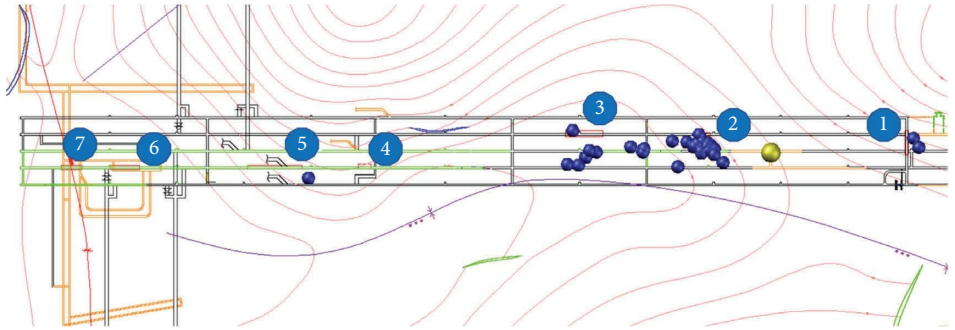

Figure 9: Microseismic distribution map of the main roadway area in panel 1 (2020.12).

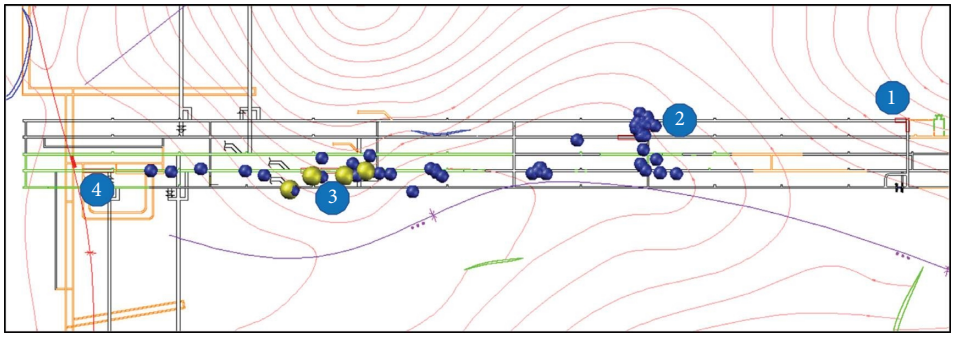

Figure 10: Microseismic distribution map of the main roadway area in panel 1 (2021.1).

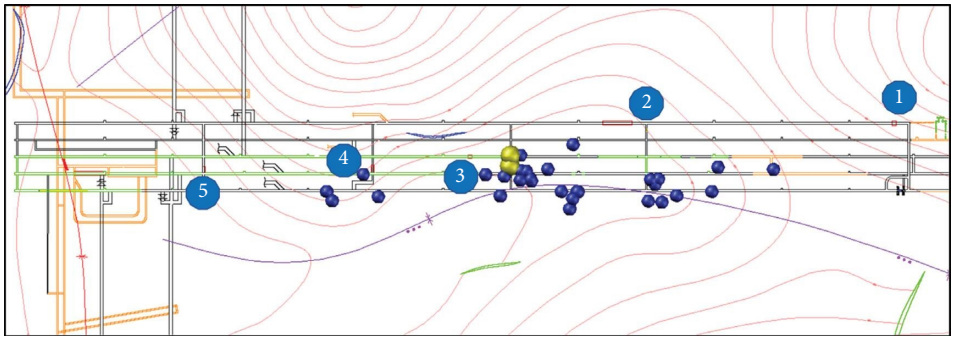

Figure 11: Microseismic distribution map of the main roadway area in panel 1 (2021.2).

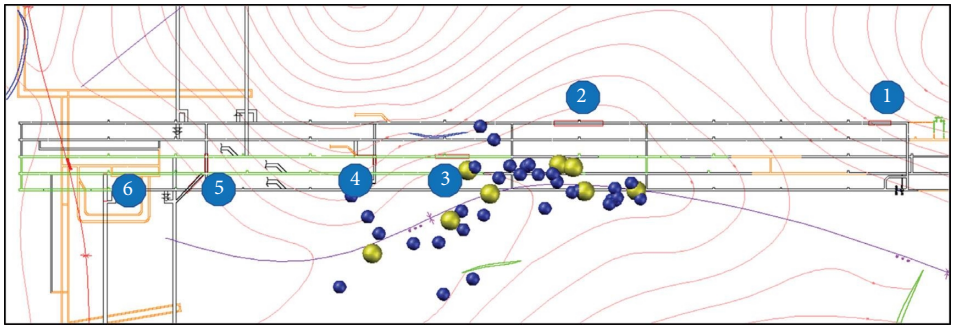

Figure 12: Microseismic distribution map of the main roadway area in panel 1 (2021.3).

average daily footage of 19 m. During this period, a total of 42 microseisms with energy greater than 10^3 J occurred, with an average of 0.071 high energy ($>10^3$ J) microseisms per meter of footage and an average of 1.35 daily high energy microseisms.

From the abovementioned statistics, it can be seen that during the tunneling of the main roadway in the panel 1 area of Xinzhuang Coal Mine, the microseismic activity basically occurs near the excavation head, and it is easy to have large energy microseismic events when the heading head and the tectonics area are in the same area. At the same time, a certain distance should be maintained between multiple excavation heads to avoid overlapping dynamic load disturbances. In summary, it can be concluded that the excavation strength has a significant impact on the occurrence of rockbursts in Xinzhuang Coal Mine.

4. Quantification of Rockburst Factors

There are various factors that affect rockburst during tunnel excavation, including geological conditions such as coal seam thickness, burial depth, and fold structure, as well as excavation technology conditions such as excavation speed and excavation method. From the analysis of local areas, there are geological conditions such as local fault structures and collapse columns, as well as technical conditions such as roadway layout and coal pillar retention. At present, Xinzhuang Coal Mine is carrying out excavation work for the main roadway of panel 1. Therefore, starting from the actual engineering background, this chapter quantifies the factors affecting rockbursts from the overall analysis during the excavation period of the main roadway.

4.1. Analysis of the Main Influencing Factors on the Impact of Roadway Excavation. Four geological influencing factors, including burial depth, fold structure, coal seam thickness and its changes, and hard overlying rock, as well as technical influencing factors such as roadway layout and excavation strength, were selected in the main roadway area of panel 1 of Xinzhuang Coal Mine, and a distribution cloud map of each factor was drawn.

4.1.1. Burial Depth. As shown in Figure 13, the burial depth of the main roadway in panel 1 of Xinzhuang Coal Mine is between 690 and 900 m and the burial depth of the seismic distribution area is between 760 and 810 m. Compared with the overall burial depth of Xinzhuang Coal Mine, the burial depth of the mining pressure manifestation area is relatively small. At the same time, from the spatial distribution characteristics of microseisms, it can be seen that there is no obvious correlation between the distribution of mining earthquakes in this area and the burial depth, so the burial depth factor in this area has a relatively small impact on the rockburst.

In addition, for the three areas where the mining pressure is more obvious, the burial depth range is between 760 and 820 m, which is relatively small compared to the overall burial depth of the main roadway area. Moreover, the distribution of mining earthquakes in this area is not significantly correlated with the burial depth. Therefore, it can be considered that the influence of burial depth factors on the mining pressure in this area is relatively small.

4.1.2. Fold Structure. The fold structure in the main roadway area of panel 1 is relatively developed, and there are three fold structures with different curvatures, namely, the S6 syncline, S7 anticline, and Qiaojiamiao syncline, located in the west, east, and north of the main roadway. Among them, the S6 syncline is nearly parallel to the direction of the main roadway and closest to it. Considering the complexity of the superposition of influencing factors, the fold distribution has been simplified. Figure 14 shows the distribution of regional fold structures and the positioning cloud map of high-energy mining earthquakes ($>10^4$ J). The positioning results indicate that mining earthquakes are frequent near the S6 syncline axis and the distribution of mining earthquakes is negatively correlated with the distance from the S6 syncline axis. Compared with the influence of the S6 syncline structure, the influence of the other two-fold crankshafts on the distribution of mining earthquakes is relatively light. Overall, the fold structure has a significant impact on the rockburst risk during the excavation of the main roadway.

From Figure 14, it can be seen that the S6 syncline axis parallel passes through the corresponding mining pressure display area of the 3~4 connecting tunnels. The distance between the mining pressure display area of the 2~3 connecting tunnels and the S6 syncline is 4~270 m, which is easily affected by the S6 syncline. The 6~7 connecting alley is almost vertically crossed by the Qiaojiamiao syncline, and the stress concentration in these areas is high due to the influence of the fold structure. Therefore, the fold structure is an important reason for the occurrence of mineral pressure in this area.

4.1.3. Coal Seam Thickness and Its Changes. Figure 15 shows the cloud map of the occurrence of coal seam thickness in the main roadway area of panel 1. It can be seen that the variation of coal seam thickness in the area is relatively uniform, with coal seam thickness ranging from 2 to 12 m. According to statistics, the distribution of mining earthquakes in areas with coal seam thickness greater than 10 m accounts for 23.9% (34 occurrences) of the total number of mining earthquakes, with the focus mainly on the 4# connecting roadway. The distribution of mining earthquakes in areas with a coal seam thickness of 5–10 m accounts for 47.8% (68 occurrences) of the total number of mining earthquakes. The distribution is relatively concentrated in the connecting roadway, while the distribution of mining earthquakes in areas with a coal seam thickness of less than 5 m accounts for 28.3% (40 occurrences) of the total number of mining earthquakes. The distribution of mining earthquakes is concentrated in the intersection area of the underground parking lot roadway. Overall, mining earthquakes are distributed in various coal-thickness regions, and their proportions are relatively close. Therefore, it can be seen that the influence of coal seam thickness and

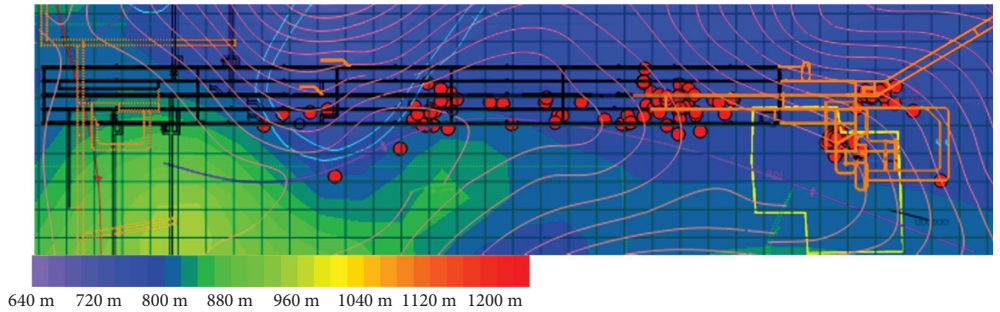

Figure 13: Cloud chart of burial depth distribution.

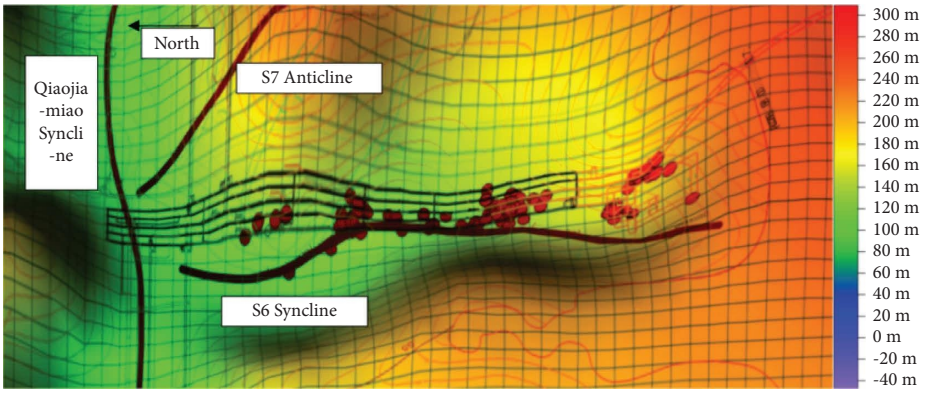

Figure 14: Three-dimensional sketch map of regional tectonics (contour line is the elevation of coal 8).

changes in mining earthquakes or rockbursts in different regions is not significantly different and its relationship with the distribution of mining tremors is not significant.

From Figure 15, it can be seen that the coal seam thickness in the three areas with obvious rock pressure manifestation is relatively large, ranging from 8 to 12 m. However, the coal seam thickness changes in this area are relatively gentle, and there is no significant change in thickness. For thick coal seams, as the thickness of the coal seam increases, the likelihood of rockburst damage occurring in front of the working face gradually increases. Therefore, it can be considered that the thickness of coal seams has a certain impact on the occurrence of rock pressure in the area.

4.1.4. Hard Overlying Rock. Figure 16 shows a cloud map of the thickness of hard rock layers with a thickness >10 m in the main roadway area of panel 1. The thickness range of the overlying hard rock layers in the area is 12–21 m, and the thickness range of the overlying hard rock layers in the mining earthquake coverage area is 14–18 m. From Figure 15, it can be seen that the distribution of mining earthquakes does not exhibit a certain regularity with the variation of the thickness of the overlying hard rock layers.

Figure 17 shows the cloud map of the distance between the hard rock layer with a thickness >10 m and the coal 8 in the main roadway area of panel 1. It can be seen from the figure that during this period, the distribution of mining earthquakes in the main roadway area of panel 1 shows a negative correlation with the distance between the overlying thick sandstone and the coal seam, that is, as the distance between the coal seam and the overlying thick sandstone decreased, the occurrence of mining earthquakes became increasingly dense and frequent. Therefore, the rockburst risk of the overlying thick sandstone layer on the main roadway area of panel 1 is relatively obvious.

From Figures 16 and 17, it can be seen that the thickness of the overlying sandstone layer in the three areas where the rock pressure is more obvious is at an average level, ranging from 12 to 19 m. However, the distance between the coal 8 layer and the thick sandstone layer in this area is relatively high, mostly concentrated within 30 m, and some of the apparent positions are even within 20 m. By combining the distribution characteristics of mining earthquakes, it can also be seen that the distribution of high-energy mining earthquakes is mostly concentrated in these areas. Therefore, it can be considered that the distance between the overlying hard rock layer and the coal layer has a significant impact on the rock pressure behavior in this area.

4.1.5. Roadway Layout. The main roadways in panel 1 of Xinzhuang Coal Mine are all coal seam tunnels, among which the return air, auxiliary transportation, and adhesive tape tunnels are all arranged in the coal seam. The design of the return air main tunnel is arranged along the coal seam roof, and the auxiliary transportation and adhesive tape main tunnels are arranged along the floor (the design of the tunnel floor leaves a 1.5 m thick coal skin). In the actual

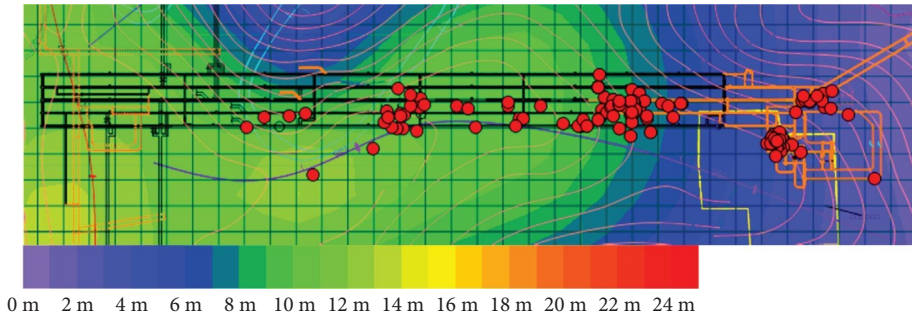

Figure 15: Cloud map of coal thickness.

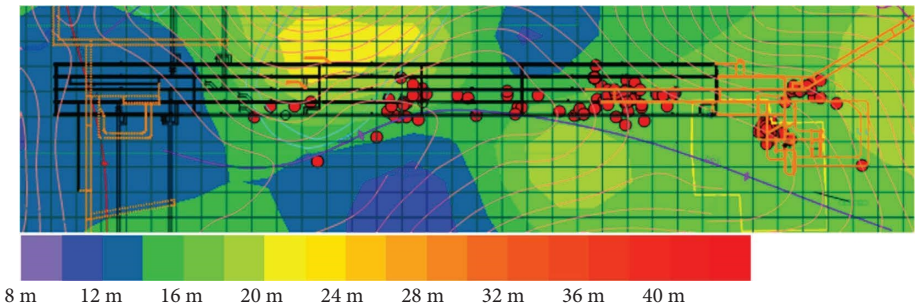

Figure 16: Cloud map of hard rock layer thickness (thickness >10 m).

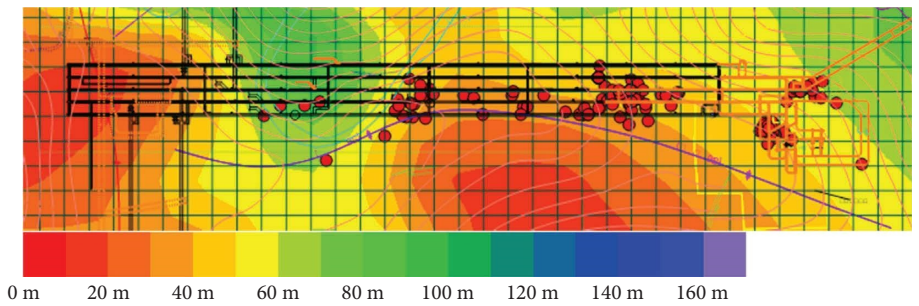

Figure 17: Cloud map of the distance between the overlying hard rock layer and the coal 8 layer.

construction process, due to the influence of geological conditions and construction technical conditions, the thick bottom coal is often left in local areas. The theoretical research and practice of rockburst indicate that when rockburst occurs, it is generally accompanied by severe floor heave and the retention of thicker bottom coal often promotes the occurrence of rockburst. For the surrounding rock of the roadway, the roof and roadway sides are generally supported, while the floor is generally unsupported, resulting in the floor becoming the weakest area of the roadway. When the rockburst pressure load acts on the surrounding rock of the tunnel, the energy will also break through from the weakest link, and this process will inevitably be accompanied by slow floor heave or sudden failure of the floor.

Figures 18–22 show the bottom coal reserve in the main roadway area of Xinzhuang Coal Mine based on the contour map of coal thickness and the statistics of coal exploration data in the main roadway.

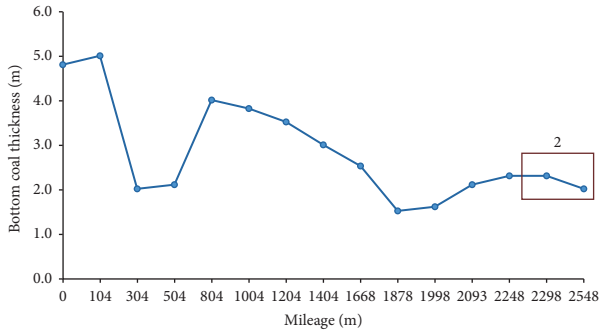

Figure 18: Bottom coal distribution curve of central west return air roadway.

It can be seen that the thickness of the bottom coal reserve in the five main roadways mostly fluctuates within the range of 1.5~2.5 m, with a relatively large thickness, and some areas even exceeding 4 m. The main roadway area is

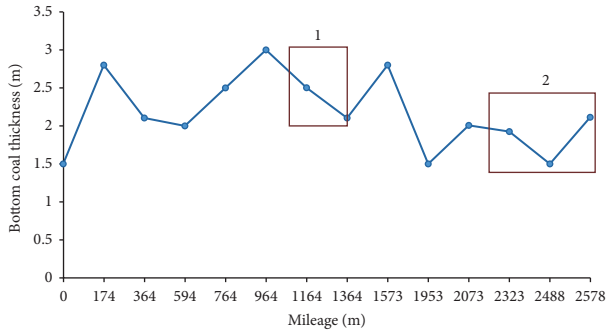

Figure 19: Bottom coal distribution curve of central west auxiliary transportation roadway.

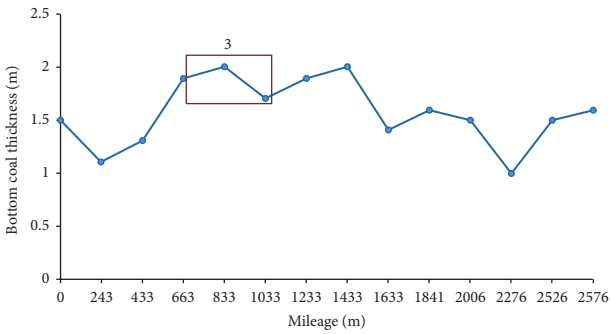

Figure 20: Bottom coal distribution curve of central belt roadway.

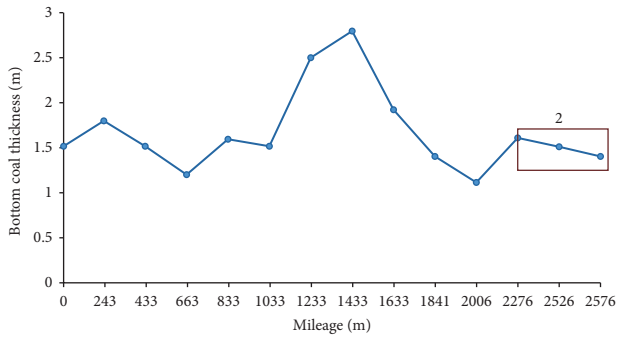

Figure 21: Bottom coal distribution curve of central east auxiliary transportation roadway.

different from the solid coal area and the roof and floor area, and it has more intuitive observation conditions. The main roadway area of Xinzhuang Coal Mine has experienced three occurrences of roadway damage caused by rock pressure manifestation, namely, the three failures counted in Table 4, which are also shown in the red border area in Figures 18–22. The red border area in the figure shows the thickness of the bottom coal reserve in the mining pressure display area, and it can be seen that thicker bottom coal is prone to instability and damage under mining earthquake disturbance, and there is a high risk of rockburst during the excavation process.

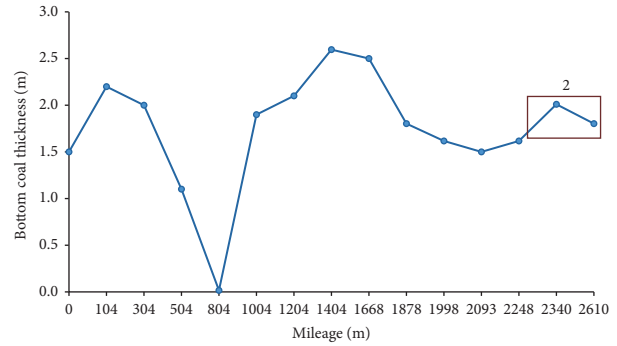

Figure 22: Bottom coal distribution curve of central east return air roadway.

4.1.6. Excavation Strength. The monthly excavation footage and microseismic conditions during the excavation period of the main roadway in panel 1 of Xinzhuang Coal Mine from December 2020 to May 2021 are shown in Figures 23 and 24. The excavation speed is the highest from April to May, with a maximum excavation volume of 1846.9 m within two months, averaging 30.8 m per day. In addition, the distance between the main tunnels of Xinzhuang Coal Mine is 50 m, and multiple excavation operations are prone to superimpose impacts, thereby increasing the risk of rockbursts. However, from the figures, it can be seen that there is no significant positive correlation between excavation intensity and mining seismic activity. Through analysis, the reason may be that there were fewer high-energy microseismic events during the excavation of the main roadway in panel 1 of Xinzhuang Coal Mine, especially during the period from December 2020 to May 2022, with only 17 high-energy events. Therefore, the data are susceptible to significant deviation and credibility is poor due to other factors. According to previous research, the dynamic load disturbance generated by excavation causes a redistribution of stress in the coal rock mass, thereby affecting the original rock stress field. The static load effect of the supporting stress field is superimposed, and then under the dynamic load disturbance of excavation, rockburst disasters occur. The dynamic load generated by excavation activities is often a starting factor for the occurrence of mining pressure. Therefore, the impact of the excavation strength of the main roadway in panel 1 on the rockburst risk cannot be ignored.

4.2. Quantification of Impact Factors

4.2.1. Steps of Analytic Hierarchy Process. Based on the analysis of the influencing factors of the rockburst mentioned above, it can be determined that the overall influencing factors are coal seam burial depth, coal seam thickness, and hard overlying rock, while the local influencing factors are excavation strength, fold structure, and roadway layout. Based on the influence range and occurrence changes of various factors, the working face is divided into regions with local influencing factors as the main factor and overall influencing factors taken into account.

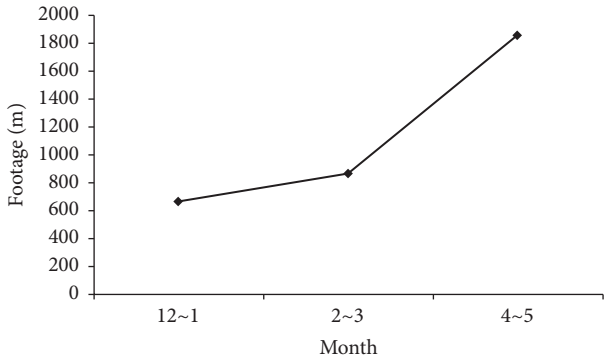

Figure 23: Monthly footage of the main roadway in panel 1.

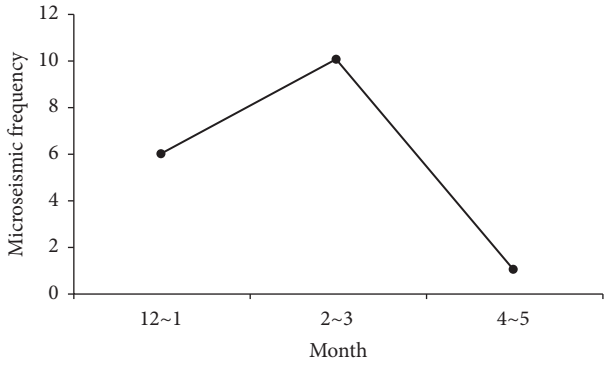

Figure 24: Monthly microseismic frequency of the main roadway in panel 1.

(1) Construct Judgment Matrix and Calculate Weight Vector. By adopting a single hierarchical model structure, the model consists of a target C and n evaluation elements $A_1, \ldots, A_n$, and evaluators that belong to it [30, 31]. By using the 1~9 scale method for relative comparison between each two elements, we construct a judgment matrix based on pairwise scale comparison as follows:

$$A\begin{bmatrix} \frac{A_1}{A_1} & \frac{A_1}{A_2} & \cdots & \frac{A_1}{A_n} \\ \frac{A_2}{A_1} & \frac{A_2}{A_2} & \cdots & \frac{A_n}{A_n} \\ \vdots & \vdots & \ddots & \vdots \\ \frac{A_m}{A_1} & \frac{A_m}{A_2} & \cdots & \frac{A_m}{A_n} \end{bmatrix} = \left[\begin{bmatrix} A_{11} & A_{22} & \cdots & A_{1n} \\ A_{21} & A_{22} & \cdots & A_{21} \\ \vdots & \vdots & \ddots & \vdots \\ A_{m1} & A_{m2} & \cdots & A_{mn} \end{bmatrix}\right]. \quad (2)$$

By using $AW = \lambda_{\max} W$, we calculate the maximum characteristic root $\lambda_{\max}$ and find its corresponding feature vector W, which is the ranking weight of each factor in the same layer corresponding to the relative importance of a certain factor in the previous layer. Then, we perform consistency testing and finally, obtain the weight matrix.

Usually we solve λmax and W using the square root method. First, we calculate the product M_i of each row of elements and then calculate the n-th root of $\overline{W_i}$. We then normalize it to obtain W_i and the weight vectors of each factor. The calculation formula is as follows:

$$\begin{aligned} M_i &= \prod_{j=1}^{n} A_{ij}, \\ \overline{W_t} &= \sqrt[n]{M_i}, \\ W_i &= \frac{\overline{W_i}}{\sum_{t=1}^{m} \overline{W_t}}, \\ \lambda_{\max} &= \sum_{i=1}^{n} \frac{(AW)_i}{W_i}. \end{aligned} \quad (3)$$

(2) Consistency Check. After finding the maximum feature root $\lambda_{\max}$, a consistency check is also required, as it is used to calculate the consistency ratio CR as follows:

$$\mathrm{CR} = \frac{\mathrm{CI}}{\mathrm{RI}} = \frac{\lambda_{\max} - n}{(n-1)\mathrm{RI}}, \quad (4)$$

where n represents the order of the average judgment matrix and RI represents the average random consistency indicator.

When CR < 0.1, it is generally believed that the consistency of the judgment matrix is acceptable, otherwise it is necessary to readjust the element weights to comply with the consistency test.

4.2.2. Area Division Based on Risk Factors. The division results of the main roadway area in panel 1 of Xinzhuang Coal Mine are shown in Figure 25, and the main division basis is as follows:

(1) Zone I is mainly affected by the burial depth of coal seams, roadway layout, excavation strength, and thick sandstone layers. This area is the underground parking lot area, with a burial depth of 760–800 m. The tunnels intersect more vertically and horizontally, and the distance between multiple excavation heads is closer, resulting in stronger disturbance effects and easier triggering of rockbursts. The thickness of the overlying sandstone layer in this area is about 18 m, which is relatively thick. Therefore, the vicinity of the well-bottom parking lot is divided into zone I.

(2) Zone II is mainly affected by the burial depth of coal seams, roadway layout, excavation strength, fold structure, close-range sandstone layers, and thick sandstone layers. This area is the main area of five main roadway layouts, with burial depths ranging from 750 to 810 m. Except for two central return air main roadways that are excavated along the coal seam roof, the other three main roadways are all excavated along the coal seam floor, with high excavation intensity. Since the distance from the fold crankshaft is 0–20 m, the thickness of the overlying sandstone layer in this area is 15–21 m, and the

distance between the coal 8 layer and the thick sandstone layer is 30–80 m, so this area is divided into zone II.

(3) Zone III is mainly affected by the burial depth of coal seams, roadway layout, excavation strength, close-range sandstone layers, thick sandstone layers, and folded structures. The burial depth is between 750 and 880 m, and the tunnels intersect more. The thickness of the overlying thick sandstone layer is 12–17 m, and the distance between the coal 8 layer and the thick sandstone layer is 15–70 m. The distribution of mining earthquakes has decreased compared to the other two areas, and this area is classified as zone III.

4.2.3. Quantification of Risk Factor Weights. Based on the correlation between the influencing factors in each area and the distribution of mining earthquakes, as well as the comparison scaling criteria by using the analytic hierarchy process, a judgment matrix for the influencing factors in each region is provided (shown in Tables 5–7).

Zone I judgment matrix can be calculated to $\lambda max = 4.010358937$, $CI = 0.003452979$, $RI = 0.89$, $CR = 0.003879752 < 0.1$. Calculation result is meeting the consistency test, then the weight matrix of coal seam burial depth, sandstone layer thickness, roadway layout, and excavation strength is $W = [0.141, 0.141, 0.263, 0.455]$.

Zone II judgment matrix can be calculated to $\lambda max = 6.313316367$, $CI = 0.062663273$, $RI = 1.26$, $CR = 0.049732757 < 0.1$. Calculation result is meeting the consistency test, then the weight matrix of coal seam burial depth, sandstone layer thickness, thick sandstone layer distance, roadway layout, excavation strength, and fold structure is $W = [0.061, 0.112, 0.112, 0.213, 0.213, 0.287]$.

Zone III judgment matrix can be calculated to $\lambda max = 6.061316617$, $CI = 0.012263323$, $RI = 1.26$, $CR = 0.009732796 < 0.1$. Calculation result is meeting the consistency test, then the weight matrix of coal seam burial depth, sandstone layer thickness, fold structure, thick sandstone layer distance, roadway layout, and excavation strength is $W = [0.061, 0.107, 0.178, 0.178, 0.178, 0.299]$.

By using the analytic hierarchy process combined with the microseismic activity of the main roadway in panel 1 of Xinzhuang Coal Mine, the weight differences of the risk main control factors in different areas were quantitatively analyzed. The research findings are as follows:

(1) The analysis shows that the main control factors of rockburst risk in Xinzhuang Coal Mine include coal seam burial depth, coal seam thickness, sandstone layer thickness, distance between thick sandstone layers, roadway layout, fold structure, and excavation strength. The area of rock pressure manifestation is mainly affected by fold structure, coal seam thickness, distance between thick sandstone layers, roadway layout, and excavation strength.

(2) The risk factors in different mining areas and the distribution of microseisms during the mining process were used to classify the risk areas. The main roadway area was divided into three sections: zone I is the bottom yard area, zone II is the main area of the main roadway, and zone III is the end area of the main roadway.

(3) The analytic hierarchy process was used to determine the weight of the risk factors within the divided impact hazard areas, and the main control factors for impact hazards are determined as follows:

Zone I: it is mainly affected by the depth of coal seam burial, thickness of the sandstone layer, roadway layout, and excavation intensity. By comparing the weight differences of these four influencing factors, it can be seen that the excavation intensity has the strongest impact on the distribution of mining earthquakes. Therefore, the main controlling factor in this area is excavation intensity.

Zone II: it is mainly influenced by the burial depth of coal seams, thickness of sandstone layers, distance between thick sandstone layers, roadway layout, excavation strength, and fold structures. By comparing the six influencing factors with the correlation between the distribution of mining and earthquakes, it can be concluded that fold structures have the strongest impact on the distribution of mining earthquakes. Therefore, the main controlling factor in this area is fold structures.

Zone III: it is mainly influenced by the burial depth of coal seam, thickness of sandstone layer, fold structure, distance between thick sandstone layers, roadway layout, and excavation intensity. By comparing the six influencing factors with the correlation between mining and earthquake distribution, it can be concluded that the excavation intensity has the strongest impact on mining earthquake distribution. Therefore, the main controlling factor in this area is excavation intensity.

5. Analysis of Rock Burst Types and Mechanisms

5.1. Analysis of Static Load Source

5.1.1. Structural Stress Analysis

(1) The Influence of Fold Structure. According to the exploration results, it was found that the fold structure in Xinzhuang Coal Mine is relatively developed. During the excavation of the main roadway, it passes through the area of the syncline axis multiple times, as shown in Figure 26, which is the stress concentration range near the fold of the main roadway excavation. As shown in the figure, the maximum stress concentration coefficient can reach up to 1.5 and the stress level in the fold axis is significantly higher than that of the other areas. The stress level in the fold wing towards the fold axis area shows an upward trend. When the main roadway excavation is pushed from the wing towards the axis, the stress level of the coal body in front will further increase. When the limit of the stress level of the rockburst is exceeded, it will cause burst manifestation. In addition, it can be seen from Figure 26 that the stress concentration degree is different along the extension direction of the fold, which indicates that the stress distribution characteristics in

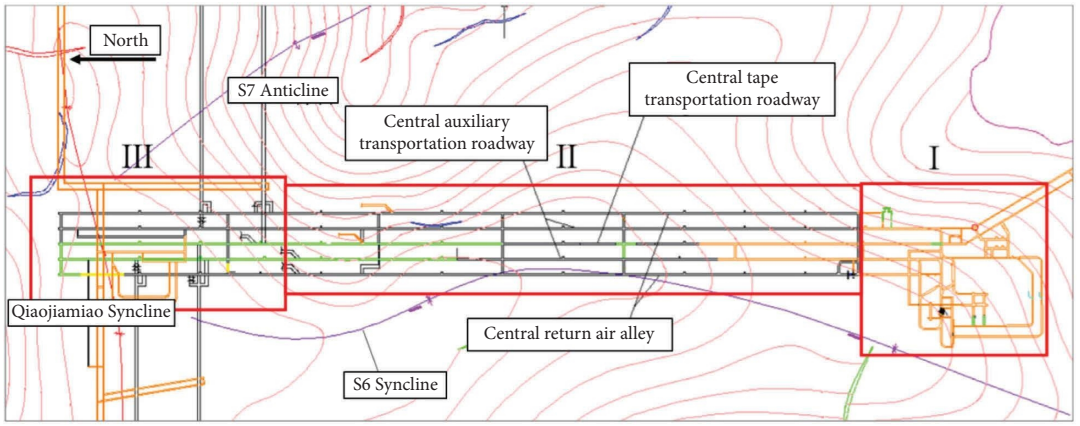

Figure 25: Division results of the main roadway area in panel 1.

Table 5: Judgment matrix of influencing factors (zone I).

C	Coal seam burial depth	Sandstone layer thickness	Roadway layout	Excavation strength
Coal seam burial depth	1	1	1/2	1/3
Sandstone layer thickness	1	1	1/2	1/3
Roadway layout	2	2	1	1/2
Excavation strength	3	3	2	1

Table 6: Judgment matrix of influencing factors (zone II).

C	Coal seam burial depth	Sandstone layer thickness	Distance to thick sandstone layer	Roadway layout	Excavation strength	Fold structure
Coal seam burial depth	1	1/2	1/2	1/3	1/3	1/4
Sandstone layer thickness	2	1	1	1/2	1/2	1/2
Distance to thick sandstone layer	2	1	1	1/2	1/2	1/2
Roadway layout	3	2	2	1	1	1
Excavation strength	3	2	2	1	1	1
Fold structure	4	2	2	2	2	1

Table 7: Judgment matrix of influencing factors (zone III).

C	Coal seam burial depth	Sandstone layer thickness	Fold structure	Distance to thick sandstone layer	Roadway layout	Excavation strength
Coal seam burial depth	1	1/2	1/3	1/3	1/3	1/4
Sandstone layer thickness	2	1	1/2	1/2	1/2	1/2
Fold structure	3	2	1	1	1	1/2
Distance to thick sandstone layer	3	2	1	1	1	1/2
Roadway layout	3	2	1	1	1	1/2
Excavation strength	4	2	2	2	2	1

different directions and regions of the fold may still differ greatly due to the differences in the heterogeneity of coal and rock mass, the development characteristics of the fold, and the local crustal stress field, which also proves the zoning characteristics of the fold under the guidance of the horizontal stress field.

(2) The Impact of Fault Structures. Fault is one of the widely existing structures in the geological bodies. When affected by stratum movement, differences of the local crustal stress field, and heterogeneity of coal and rock mass, a high-stress area is often formed near the fault. The stress concentration during the excavation of the main roadway under the influence of faults is shown in Figure 27. As shown in the figure, the maximum stress concentration coefficient can reach up to 1.3. The stress level in the fault development area is significantly higher than that in other areas, and the stress concentration degree in the middle area of the fault is significantly higher than that in its end area. This reminds us to try to avoid

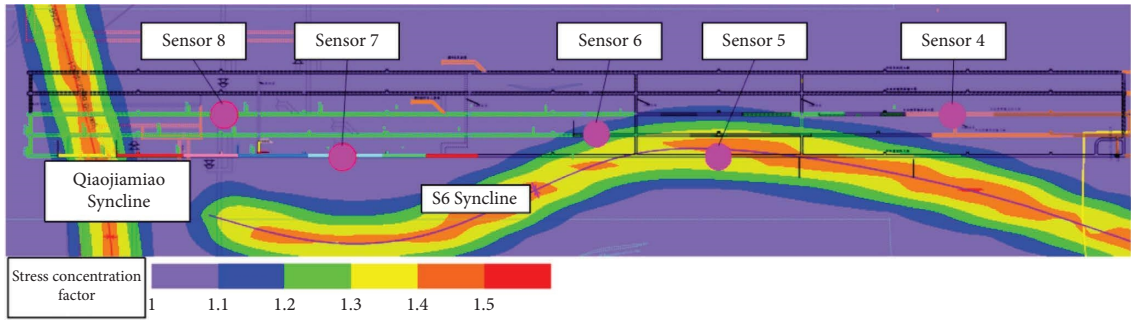

Figure 26: Stress concentration factor caused by folds.

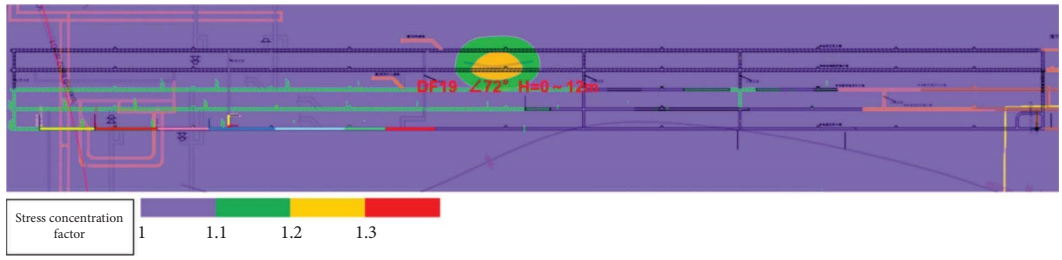

Figure 27: Relative stress concentration caused by the influence of fault structure.

directly passing through the middle of the fault during tunnel excavation, which can reduce the impact of fault structural stress to a certain extent.

5.1.2. Analysis of Support Pressure. Xinzhuang Coal Mine has a large burial depth, thick coal seam, large excavation space, and hard overburden, and the support pressure value of excavation is relatively high and has a significant impact range. Combined with the ground stress test result in Table 1, the static load performance of abutment pressure is mainly crustal stress based on horizontal stress.

5.2. Rockburst Dynamic Load Source Analysis. During the excavation period of Xinzhuang Coal Mine, the main source of dynamic load came from excavation activities, which is closely related to the occurrence of mining earthquakes. In general, when the seismic energy of the mine is less than 10^7 J, the seismic load transmitted to the main roadway or working face coal seam is relatively small, generally not exceeding 10 MPa. According to the microseismic data of Xinzhuang Coal Mine, the maximum energy of the mining earthquake during the excavation of the five main tunnels is 10^4 J level, which means that the dynamic load of the seismic source will not exceed 10 MPa. The distribution of 10^4 J level seismic sources during the excavation period is shown in Figure 28.

In summary, according to the development profile of the Xinzhuang Coal Mine, the buried depth of the main roadway is 716~940 m and the vertical stress is about 17.9~23.5 MPa. According to the static load calculation formula, the maximum static load of the main roadway under normal excavation conditions is about 30.55 MPa. When encountering special tectonics or abutment pressure influence area, the maximum static load is about 48.83 MPa. It can be seen that the static load is close to the minimum stress of 70 MPa where the rockburst occurs. In addition to the superposition of dynamic load, the possibility of rockburst disaster has objectively existed.

5.3. Mechanism and Types of Potential Rock Burst. The main mechanical properties of coal rock mass are strong compressive strength and weak tensile strength, so it accumulates a lot of energy caused by pressure during the stress process, which is static load pressure. However, at the same time, coal and rock masses (especially coal bodies) generally have brittleness, especially when subjected to dynamic load disturbances, the mechanical state changes and the load-bearing capacity changes, making it easier to highlight this property, namely, dynamic load disturbances. In practical engineering, the superposition of dynamic and static loads is a situation that is highly prone to causing rockburst disasters. The excavation process can lead to a redistribution of stress in the surrounding rock. Under high static load conditions, the surrounding rock accumulates a large amount of energy, which can easily break this fragile equilibrium state after mining disturbance, namely, dynamic load-induced and high static load energy storage-induced rockburst disasters.

Based on the previous research and analysis, the scope of mining activities in Xinzhuang Coal Mine is currently small (only for main roadway excavation) and the dynamic load generated by mining disturbance is limited. However, the large burial depth, support pressure, thicker bottom coal, and fold and fault structures in the Xinzhuang Coal Mine cause a sharp increase in the static load

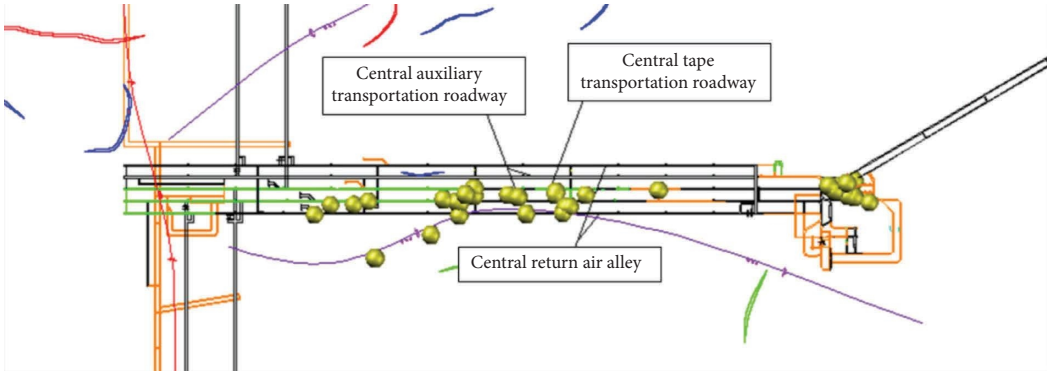

Figure 28: Distribution of 10^4 J level seismic sources during excavation.

level in the excavation area. Therefore, when the high static load in the coal and rock body exceeds its failure critical value under dynamic load disturbance to induce burst behavior, static load stress dominates and dynamic load plays a disturbance role. Therefore, the type of potential rockburst during the excavation of Xinzhuang Coal Mine is currently the "high static load and dynamic load disturbance" type.

6. Conclusion

Through basic data analysis and theoretical derivation, this study reveals the mechanism and main influencing factors of rockburst under complex conditions of large buried depth, thick topsoil, and hard overburden in Xinzhuang Coal Mine. The main conclusions are as follows:

(1) The research has determined that the main factors causing rockburst disasters in Xinzhuang Coal Mine are mining depth, coal seam thickness, changes in coal seam thickness, tectonic stress field, hard overlying rock, roadway layout, bottom coal retention, and excavation activities. Xinzhuang Coal Mine is mainly mining coal 8 layer; during the tunneling of the main roadway in panel 1, the microseismic activity basically occurs near the heading head and it is easy to have large energy microseismic events when the heading head is in the same area as the tectonics area.

(2) The study analyzed the reasons for the occurrence of rock pressure during the excavation process of the main roadway and quantified the weight of each factor. The excavation process of the main roadway in Xinzhuang Coal Mine is mainly influenced by the depth of coal seam, thickness of coal seam, thickness of sandstone layer, distance between thick sandstone layers, roadway layout, fold structure, and excavation strength. The risk factors of rockbursts in different mining areas and the distribution of microseisms during the mining process were used to classify the risk areas of rockbursts in the working face. The analytic hierarchy process was used to determine the weight of the risk factors within the divided impact hazard areas.

(3) It revealed the mechanism of potential rockburst in Xinzhuang Coal Mine. The key to the occurring process of rockburst disaster in Xinzhuang Coal Mine lies in the superimposed influence of static and dynamic loads on the surrounding rock system of the tunnel. Considering that the high burial depth, support pressure, thick bottom coal, and fold/fault structures of the Xinzhuang Coal Mine cause a sharp increase in static load levels in the excavation and mining areas, the potential type of rockburst during the excavation, and the mining period of Xinzhuang Coal Mine is a "high static load and dynamic load disturbance" type.

The research focus of this study is on the mechanism and main influencing factors of rockbursts in Xinzhuang Coal Mine. On this basis, the geological occurrence conditions and mining technical conditions of Xinzhuang Coal Mine's mining face, combined with mine area prevention measures, and based on the principle of "local follow-up, zoning management, and classified prevention and control," comprehensive prevention and control technical measures of "roof-coal seam-floor" can be developed for zoning, classification, and grading of mining working faces and other areas (such as large diameter drilling pressure relief, roof blasting, and water pressure to crack), and timely adjustment and optimization based on actual rock pressure manifestation and inspection of the control effect of rockburst which can provide important support for the prevention and control of rockburst in Xinzhuang Coal Mine. In the future, we will continue to follow up on the prevention and control of rockbursts in Xinzhuang Coal Mine and continue to pay attention to advanced directions such as filling mining, entry retaining, and intelligent monitoring under rockburst conditions [32, 33].

Data Availability

The data used to support the findings of the study are available from the corresponding author upon request.

Conflicts of Interest

The authors declare that they have no conflicts of interest.

Authors' Contributions

During the preparation and writing of this manuscript, Ma Xingen, Pan Jun, and Zou Qinghai played an important role in methodology, validation, writing, and formal analysis. Li Yongyuan conducted a lot of investigation work. Feng Fan and Wang Huifeng provided research resources, that is, the collection and analysis of onsite monitoring raw data. Ye Xiangping and Gong Yongchun were responsible for detailed data processing and analysis. Mou Biao provided financial support for the research and was responsible for drawing images.

Acknowledgments

This research was financially supported by the State Key Laboratory for Geomechanics and Deep Underground Engineering (SKLGDUEK2020), Huaneng Group Headquarters Science and Technology Project (HNKJ21-H56-10/HNKJ20-H32), and the Coal Burst Research Center of China Jiangsu. In addition, this paper was guided by Professor Dou Linming's team of China University of Mining and Technology in research and paper writing. More importantly, the manuscript was submitted on June 9, 2023, which was also the day my daughter Ma Zhengyu was born. The authors are thankful for her arrival!

References

[1] L. Yuan, Y. Jiang, X. He et al., "Research progress of precise risk accurate identification and monitoring early warning on typical dynamic disasters in coal mine," *Journal of China Coal Society*, vol. 43, no. 2, pp. 306–318, 2018.

[2] L. Yang and C. Ding, "Fracture mechanism due to blast-imposed loading under high static stress conditions," *International Journal of Rock Mechanics and Mining Sciences*, vol. 107, pp. 150–158, 2018.

[3] S. He, X. He, D. Song et al., "Multi-parameter integrated early warning model and an intelligent identification cloud platform of rockburst," *Journal of China University of Mining and Technology*, vol. 52, no. 5, pp. 850–862, 2022.

[4] Z. Wang, P. Wang, L. Shi et al., "Research on prevention of rockburst based on stress analysis of surrounding rock of gob-side entry," *Journal of China University of Mining and Technology*, vol. 49, no. 6, pp. 1046–1056, 2020.

[5] R. Yang, C. Ding, L. Yang, and C. Chen, "Model experiment on dynamic behavior of jointed rock mass under blasting at high-stress conditions," *Tunnelling and Underground Space Technology*, vol. 74, pp. 145–152, 2018.

[6] J. Zheng, W. Ju, D. Lv et al., "Mechanism and practice of roof strip weakening method for preventing rockburst in central roadway," *Journal of China Coal Society*, vol. 48, no. 03, pp. 1169–1178, 2023.

[7] H.-W. Jin and Z.-Q. Yang, "Study on reasonable layout of upper protective layer for prevention rockburst under coal seam group with close quarters conditions," *Shock and Vibration*, vol. 2021, Article ID 6139935, 17 pages, 2021.

[8] L. Dou and X. He, *Theory and Technology of Rock Burst Prevention and Control*, China University of Mining and Technology Press, Xuzhou, China, 2001.

[9] Q. Qi and L. Dou, *Theory and Technology of Rock Burst*, China University of Mining and Technology Press, Xuzhou, China, 2008.

[10] X. Ding, X. Xiao, Y. Pan, and D. Wu, "Study on damage evolution and fracture energy of coal with different bursting liability under uniaxial compressive test," *Journal of Mining and Safety Engineering*, vol. 39, no. 3, pp. 517–526, 2022.

[11] F. Jiang, X. Zhang, and S. Zhu, "Discussion on key problems in prevention and control system of coal mine rockburst," *Coal Science and Technology*, vol. 51, no. 1, pp. 203–213, 2023.

[12] P. K. Kaiser and M. Cai, "Design of rock support system under rockburst condition," *Journal of Rock Mechanics and Geotechnical Engineering*, vol. 4, no. 3, pp. 215–227, 2012.

[13] A. Mottahedi and M. Ataei, "Fuzzy fault tree analysis for coal burst occurrence probability in underground coal mining," *Tunnelling and Underground Space Technology*, vol. 83, pp. 165–174, 2019.

[14] B. P. Simser, "Rockburst management in Canadian hard rock mines," *Journal of Rock Mechanics and Geotechnical Engineering*, vol. 11, no. 5, pp. 1036–1043, 2019.

[15] C. Yi, D. Johansson, and J. Greberg, "Effects of in-situ stresses on the fracturing of rock by blasting," *Computers and Geotechnics*, vol. 104, pp. 321–330, 2018.

[16] P. Konicek, K. Soucek, L. Stas, and R. Singh, "Long-hole destress blasting for rockburst control during deep underground coal mining," *International Journal of Rock Mechanics and Mining Sciences*, vol. 61, pp. 141–153, 2013.

[17] S.-W. Oh, B.-H. Choi, Y.-B. Jung, and S.-H. Cho, "A comparative study on the dynamic tensile strength evaluation method of rock materials," *Shock and Vibration*, vol. 2023, Article ID 3631729, 14 pages, 2023.

[18] GB/T25217.1-2010, *National Standard of the People's Republic of China-Determination of Rock Burst Tendency Standard*, Standardization Administration of China, 2010.

[19] M. Gao, Y. Zhao, X. Gao, and X. Wang, "Study on the mechanism of rockbursts caused by rock plates between subvertical extra-thick coal seams and its prevention and treatment," *Journal of Mining and Safety Engineering*, vol. 36, no. 2, pp. 298–305, 2019.

[20] S. Ma, C. Cao, and Q. Hui, "Main roof breakage and vibration induced coal burst occurring in longwall roadways," *Shock and Vibration*, vol. 2021, Article ID 4982522, 7 pages, 2021.

[21] C. Lu, H. Liu, B. Liu, and J. Fan, "Practice of rockburst dynamic prevention in deep high-stress concentration district," *Journal of China Coal Society*, vol. 35, no. 12, pp. 1984–1989, 2010.

[22] J. Liang, H. Jing, X. Li, and G. Hou, "The deformation behavior and failure modes of surrounding rock after excavation: a experimental study," *Shock and Vibration*, vol. 2023, Article ID 4727706, 19 pages, 2023.

[23] C. Wang, F. Jiang, and J. Liu, "Analysis on control action of geologic structure on rockburst and typical cases," *Journal of China Coal Society*, vol. 37, no. S2, pp. 263–268, 2012.

[24] H. Wang and X. Wang, "Prevention of rockburst technology of the steep inclined thick coal seam in Wudong Coal Mine," *Journal of Mine Automation*, vol. 48, no. S2, pp. 58–61, 2022.

[25] L. Sun and Y. Gao, "Occurrence mechanism of rockburst where coal thickness changes," *Energy technology*, vol. 18, no. 7, pp. 24–28, 2020.

[26] D. Zhang, X. Wang, W. Guo et al., "The influence of coal seam thickness on the pressure relief and energy release mechanism of large-diameter drilling hole," *Coal Science and Technology*, vol. 51, no. 7, pp. 1–11, 2023.

[27] S. Wang, A. Cao, H. Wang et al., "Mechanism of "dislocation-clamping" rockburst in steeply inclined and extra thick coal seam," *Journal of Mining and Safety Engineering*, vol. 39, no. 7, pp. 711–719+769, 2022.

[28] X. Yan, "Impact of the mining speed of the deep mine fully-mechanized working face on the mining quake disasters," *Journal of Safety and Environment*, vol. 314, no. 2, pp. 19–22, 2014.

[29] S. Hong, U. C. Han, G. C. Kim, K. M. Ri, and S. Ri, "Numerical simulation of the collision breakage process between the agglomerate and hammer in a hammer crusher using DEM," *Shock and Vibration*, vol. 2023, Article ID 2838179, 14 pages, 2023.

[30] Q. Zhu, L. Gu, Y. Cheng et al., "Design and implementation of evaluation software for coal mine rockburst prevention system," *Journal of North China Institute of Science and Technology*, vol. 19, no. 5, pp. 1–7, 2022.

[31] X. Ma, M. He, B. Hu et al., "Study on key parameter design and adaptability technology of the 110 mining method for the yuwang NO.1 coal mine in the diandong mining area," *Minerals*, vol. 13, no. 2, p. 176, 2023.

[32] A. Smoliński, D. Malashkevych, M. Petlovanyi, K. Rysbekov, V. Lozynskyi, and K. Sai, "Research into impact of leaving waste rocks in the mined-out space on the geomechanical state of the rock mass surrounding the longwall face," *Energies*, vol. 15, no. 24, p. 9522, 2022.

[33] D. Malashkevych, M. Petlovanyi, K. Sai, and S. Zubko, "Research into the coal quality with a new selective mining technology of the waste rock accumulation in the mined-out area," *Mining of Mineral Deposits*, vol. 16, no. 4, pp. 103–114, 2022.